ACS OMEGA

Open Access

http://pubs.acs.org/journal/acsodf

Article

New 1,3,4-Thiadiazole Derivatives as α-Glucosidase Inhibitors: Design, Synthesis, DFT, ADME, and In Vitro Enzymatic Studies

Zahid Ali, Wajid Rehman,* Liaqat Rasheed, Abdullah Y. Alzahrani, Nawab Ali, Rafaqat Hussain, Abdul-Hamid Emwas, Mariusz Jaremko, and Magda H. Abdellattif

Cite This: *ACS Omega* 2024, 9, 7480−7490

Read Online

ACCESS | Metrics & More | Article Recommendations | Supporting Information

ABSTRACT: Diabetes is an emerging disorder in the world and is caused due to the imbalance of insulin production as well as serious effects on the body. In search of a better treatment for diabetes, we designed a novel class of 1,3,4-thiadiazole-bearing Schiff base analogues and assessed them for the α-glucosidase enzyme. In the series (**1**−**12**), compounds are synthesized and **3** analogues showed excellent inhibitory activity against α-glucosidase enzymes in the range of IC_{50} values of 18.10 ± 0.20 to 1.10 ± 0.10 μM. In this series, analogues **4**, **8**, and **9** show remarkable inhibition profile IC_{50} 2.20 ± 0.10, 1.10 ± 0.10, and 1.30 ± 0.10 μM by using acarbose as a standard, whose IC_{50} is 11.50 ± 0.30 μM. The structure of the synthesized compounds was confirmed through various spectroscopic techniques, such as NMR and HREI-MS. Additionally, molecular docking, pharmacokinetics, cytotoxic evaluation, and density functional theory study were performed to investigate their behavior.

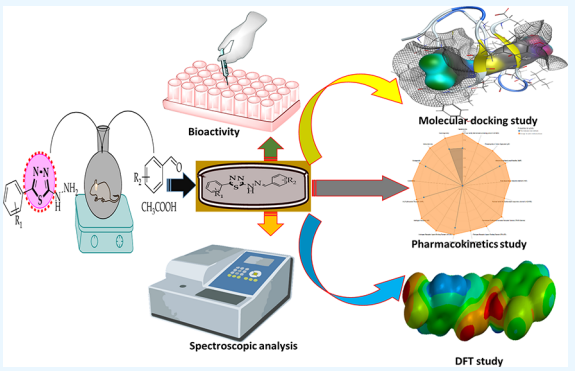

1. INTRODUCTION

Heterocyclic compounds are cyclic and contain carbon and other elements, such as oxygen, nitrogen, and sulfur. Pyrrole, furan, and thiophene belong to heterocyclic molecules with a single heteroatom, while azole, pyrrole, thiazole, thiadiazole, oxadiazole, triazene, and other heterocyclic molecules have multiple heteroatoms.[1] Heterocyclic molecules found in a wide variety of them showed significant therapeutic properties. The important feature of thiadiazole derivatives in research has recently increased due to their significant properties; thiadiazole is a versatile intermediate in medicinal chemistry and belongs to the classes of heterocycles that contain sulfur and nitrogen and are widely used in synthesizing biologically active molecules. Thiadiazole shows different isomeric forms of thiadiazole. However, 1,3,4-thiadiazole was found to be the most important in the biological and pharmacological system.[2] Due to their wide range of pharmacological properties, substituted 1,3,4-thiadiazole derivatives have had a greater interest in research in recent years.[3] Due to the presence of the N−C−S moiety, 1,3,4-thiadiazole derivatives are thought to have different biological activities.[4] Authors recommend that the 1,3,4-thiadiazole derivative's biological activities are shown due to the strong aromaticity of the ring, in vivo stability, and thiadiazole had less to zero toxicity for higher vertebrates, which includes humans for the treatment of cancer.[5,6] The aromatic five-membered ring of thiadiazole contains two nitrogen atoms and one sulfur atom. It also has a two-electron donor system and a hydrogen bonding domain, allowing it to act as an anhydrase.[7]

The 1,3,4-thiadiazole was the isomer on which we concentrated due to their properties. The various biological activities of 1,3,4-thiadiazole are antimicrobial,[8,9] antituberculosis,[10] anti-inflammatory,[11,12] carbonic anhydrase inhibitory,[13] anticonvulsant,[14,15] antihypertensive,[16,17] antioxidant,[18,19] anticancer,[20,21] and antifungal[22] properties. Drug molecules that contain 1,3,4-thiadiazole groups in their structures and their examples are given, e.g., carbonic anhydrase inhibitors acetazolamide and methazolamide.[23] The thiadiazole group was known to replace the thiazole moiety in a bioisosteric way.[24] Due to this, the strong aromaticity of thiadiazole derivatives provides them with biological activity.

Azomethine or imine functional groups are found in various compounds known as Schiff bases. Primary amines and carbonyl compounds such as ketones and aldehydes condense to form Schiff bases as well as imine bases. Due to their potency against various diseases such as analgesic, anti-inflammatory, anticonvulsant, anticancer, antimicrobial, antituberculosis, antioxidant, and anthelmintic properties, the

Received: August 9, 2023
Revised: December 14, 2023
Accepted: December 15, 2023
Published: February 5, 2024

Schiff bases have recently received attention in the medical and pharmaceutical fields.[25−28] Schiff bases are broadly used in many industrial fields as dyestuffs, pigments, catalysts, corrosion inhibitors, and polymer stabilizers in addition to their pharmacological properties.[29]

Diabetes mellitus, also known as a chronic disorder, happens due to a deficiency of insulin production in the body. Increased blood glucose levels are an emerging feature of this disease, which can harm various physiological systems, including blood vessels and nerves.[30] Type-II, which accounts for up to 95% of all cases of diabetes mellitus, is expected to increase to 578 million cases by 2030, which is an alarming situation, according to the WHO.[31] Maintaining normal glycemic levels in fasting and postprandial states is the generally accepted treatment objective for T2DM. Exercise and diet are the first goals to achieving this purpose, but oral antidiabetic pharmacotherapy is also crucial. Meglitinides and sulfonylureas belong to a class of insulin secretagogues, while aldose reductase inhibitors, insulin sensitizers, glucose absorption inhibitors (like a-glucosidase inhibitors), and the recently developed 4-dipeptidyl peptidase inhibitors are insulin sensitizers and glucose absorption inhibitors.[32] Although these medications are found to be effective for the treatment of diabetes, there is still an urgent need to develop new antidiabetic agents with greater efficiency and lower toxicity.

Previous 1,3,4-thiadiazole[33−35] and Schiff base[36−38] derivatives (Figure 1) have shown various biological activities, but in

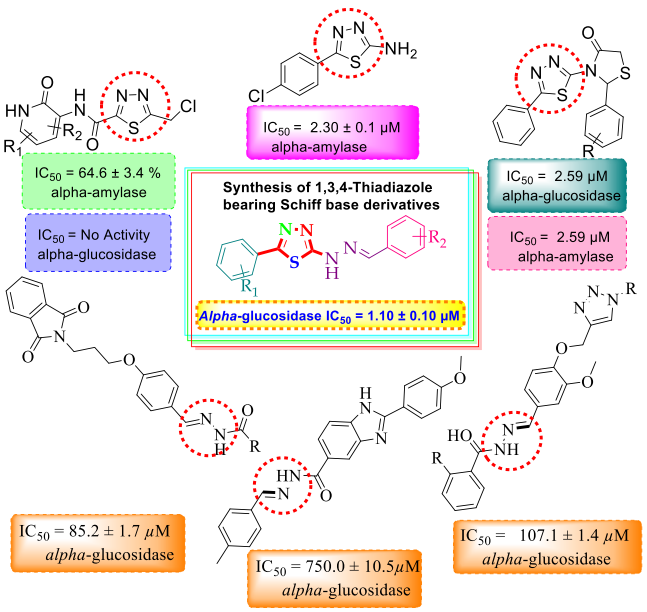

Figure 1. Rational of the current study.

current research, we will design novel routes for the synthesis of 2-hydrazine-5-(4-nitrophenyl)-1,3,4-thiadiazole-bearing Schiff base derivatives to overcome such issues[39] in the future.

2. RESULTS AND DISCUSSION

2.1. Chemistry. In the first step, $N_2H_4.H_2O$ (a) was added to carbon disulfide in MeOH, and the reaction mixture was refluxed until conversion was complete (TLC was employed to check the conversion) to form thiocarbohydrazide (b). Substrate (b) was then subjected to 4-nitro-benzaldehyde in a methanolic solution along with a few drops of CH_3COOH, and the resulting residue was stirred at refluxing temperature to produce intermediate (c), which further undergoes cyclization through an oxidative process in the presence of I_2 and K_2CO_3 in 1,4-dioxane to afford the synthesis of 2-hydrazino-1,3,4-thiadiazoles (d). In the next step, intermediate (d) was reacted with different substituted benzaldehydes in acetic acid, and the resulting mixture was stirred under reflux to access the synthesis of the desired 1,3,4-thiadiazole-based Schiff base analogues (**1**−**12**).

2.2. Biological Activity. *2.2.1. In Vitro α-Glucosidase Activity (1−12).* In this study, thiadiazole-based Schiff base analogues were afforded via oxidative C−S bond formation and evaluated *in vitro* for α-glucosidase potentials compared to acarbose as reference drugs according to the protocol in the literature. All the newly afforded scaffolds were identified to show moderate-to-good inhibitory potentials (Table 1).

Table 1. α-Glucosidase Inhibition Profile of Thiadiazole-Based Schiff Base Analogues

S. No.	Ring B	IC_{50} ±SEM[a] [μM]	S. No.	Ring B	IC_{50} ± SEM[a] [μM]
1		13.40 ± 0.30	7	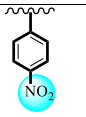	4.90 ± 0.20
2		14.80 ± 0.30	8	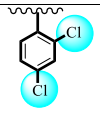	2.20 ± 0.10
3	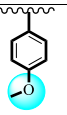	11.20 ± 0.20	9	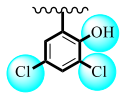	1.10 ± 0.10
4	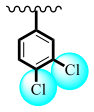	1.30 ± 0.10	10	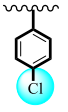	3.70 ± 0.10
5		5.40 ± 0.20	11	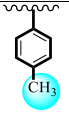	13.60 ± 0.30
6	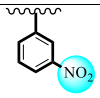	9.90 ± 0.30	12	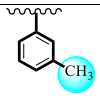	18.10 ± 0.20
Acarbose standard drug					11.50 ± 0.30 μM

[a]The IC_{50} value of standard drug acarbose is set as per the literature.[40]

The structure activity relationship (SAR) study showed that analogues that hold substituents of either strong electron donating groups (EDG) or electron with drawing (EWD) groups located at either end of the thiadiazole ring showed better inhibition profiles than analogues that bear bulky groups. In this regard, strong EWG groups attract electronic density toward themselves, making the ph-ring more susceptible to interaction with enzyme active sites through dipole−dipole interactions. Furthermore, the interaction of

https://doi.org/10.1021/acsomega.3c05854
ACS Omega 2024, 9, 7480−7490

synthesized analogues also depends on their position around the ph-ring. Among the current synthesized series, analogue **9** that holds −OH moiety and two chloro groups is shown to be the better α-glucosidase inhibitor. This better inhibition profile was due to the strong EWG effect exhibited by two −Cl groups as well as the participation of the −OH. group in H-bonding with the enzyme active site. However, the activity of this analogue **9** was altered by either replacing these −Cl and −OH groups with some other bulky groups or deattachment of these groups. Analogue **4**, having one −OH group less than analogue **9** around ph-ring, was found to show somewhat less activity than analogue **9** but identified as the second most potent analogue among the current series. This higher inhibitory potential of analogue **4** was also due to strong EWD exhibited by two −Cl groups around the ph-ring at its meta- and para-position. The two −Cl groups make the ph-ring a strong electron-deficient entity, which may help in interaction through dipole−dipole interaction with the enzyme active site (Figure 2).

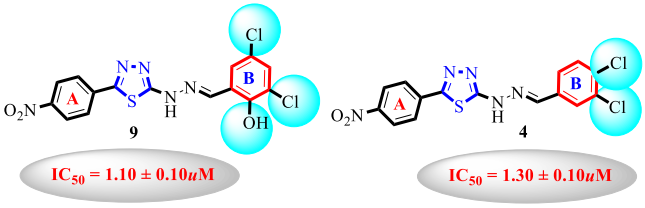

Figure 2. SAR study of most potent scaffolds **9** and **4**.

It was suggested by the SAR study that the analogues that hold −OCH_3 groups around ph-ring B located at its different position were shown to possess weak inhibition profiles against α-glucosidase enzymes and were found to be either less potent or somewhat comparable to standard drugs such as acarbose. We compared analogue **1** bearing an ortho-OCH_3 moiety at ph-ring B with analogue **2** bearing a meta-OCH_3 group at ph-ring B, and analogue **1** was known to have more potency toward α-glucosidase than analogue **2**. Similarly, if we compared analogue **1** bearing an ortho-OCH_3 moiety at ph-ring B with analogue **3** bearing para-OCH_3 group at ph-ring B, analogue **3** was known to have more potency toward alpha-glucosidase than analogue **2**. The inhibition profile was altered by shifting the −OCH_3 group from the ortho-position or meta-position of analogues **1** and **2** to the para-position as in analogue **3**. This difference in inhibition profile is shown by these analogues having −OCH_3 located at different positions of ph-ring B. Therefore, they interact differently with α-glucosidase enzymes, showing different potencies (Figure 3).

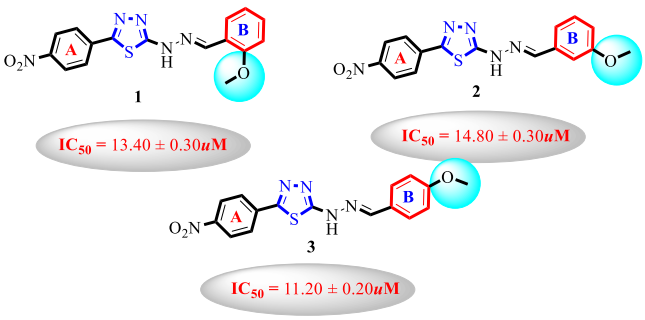

Figure 3. SAR study of analogues **1**, **2**, and **3**.

The SAR study suggests that the analogues that hold -NO_2 groups around ph-ring B located at different positions possess considerable inhibition profiles against the α-glucosidase enzyme and were found to be many fold more potent than standard drugs such as acarbose. If we compared analogue **5** bearing an ortho-NO_2 moiety at ph-ring B with analogue **6** bearing a meta-NO_2 group at ph-ring B, analogue **5** was known to have more potency toward α-glucosidase than analogue **6**. Similarly, if we compared analogue **5** bearing an ortho-NO_2 moiety at ph-ring B with analogue **7** bearing a para-NO_2 group at ph-ring B, analogue **7** was known to have more potency toward α-glucosidase than analogue **5**. The inhibition profile was altered by shifting the −NO_2 group from the ortho-position or meta-position of analogues **5** and **6** to the para-position as in analogue **7**. This difference in inhibition profile is shown by these analogues having −NO_2 located at different positions of ph-ring B. Therefore, they interact differently with α-glucosidase enzymes, showing different potencies (Figure 4).

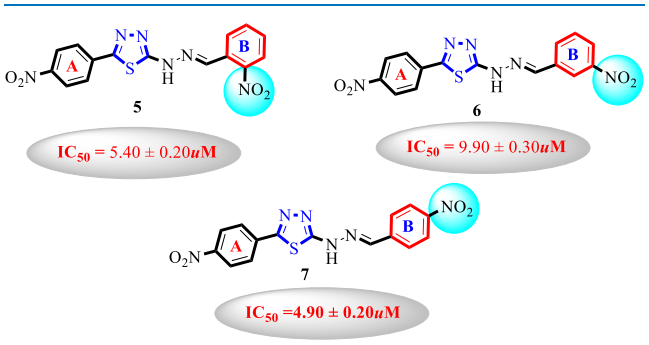

Figure 4. SAR study of analogues **5**, **6**, and **7**.

Surprisingly, it was noteworthy that the inhibition profile was enhanced by many folds by adding groups that offered a strong EWG effect, such as −Cl groups around ph-ring B. Therefore, chloro groups containing analogues were known to have promising activity through interesting interactions with enzyme active sites. By comparing analogue **10** bearing −Cl group at the para-position of ph-ring with analogue **8** which holds two −Cl groups at ortho- and para-positions of ph-ring B, analogue **8** showed better activity than analogue **10**. This increase in activity of analogue **8** compared to analogue **10** was due to the attachment of more chloro groups. Two chloro groups attract more electronic density toward itself, making the ph-ring partially positive for interaction with the enzyme active site.

Similarly, by comparing analogue **10** bearing −Cl group at the para-position of the ph-ring with analogue **4**, which holds two −Cl groups at the meta- and para-positions of the ph-ring B, analogue **4** showed better activity than analogue **10**. This elevation in activity of analogue **4** compared to analogue **10** was due to the attachment of more chloro groups around the ph-ring. However, the activity of analogue **10** was enhanced by introducing one more chloro group either at its ortho-positions or at its meta-position as in analogues **8** and **4**; therefore, it was shown that the addition of groups of the EWG nature has a significant effect on the activity. In addition, by comparing analogues having di-Cl substitutions around the ph-ring, such as **8** and **4** with the same substituents around the ph-ring, in different positions, they have different interactions with α-glucosidase (Figure 5).

https://doi.org/10.1021/acsomega.3c05854
ACS Omega 2024, 9, 7480−7490

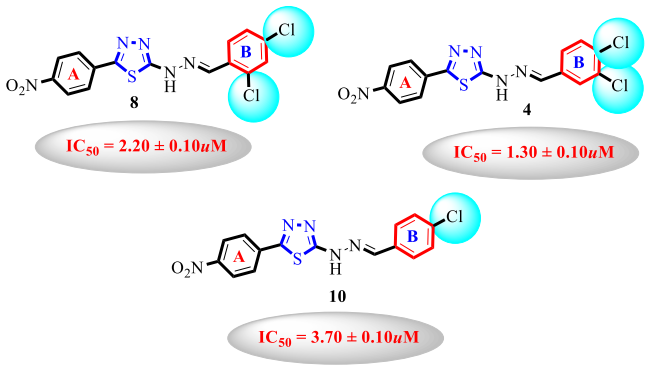

Figure 5. SAR study of analogues **4**, **8**, and **10**.

The activity of analogues having groups of either a weak EDG nature or bulky size decreased by many folds as in analogues **11** and **12**. These $-CH_3$ substituted analogues showed a weak inhibitory profile toward the α-glucosidase enzyme. They showed less potency than standard acarbose. By comparing analogue **11** bearing a para-methyl substitution with analogue **12** having a meta-methyl group, analogue **11** showed more potency than analogue **12**, but both analogues were less potent than the standard drug. However, the potency of both of these analogues was increased by many folds by removing the methyl group, followed by adding two chloro groups of EWG nature along with the hydroxyl group as in analogue **9** (Figure 6).

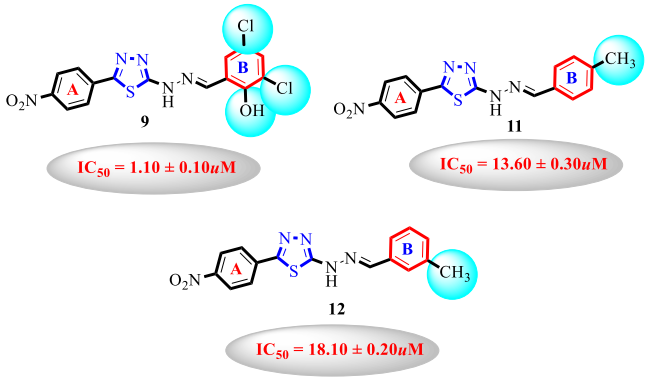

Figure 6. SAR study of analogues **9**, **11**, and **12**.

From the SAR mentioned above study, it was summarized that activity was affected by the nature, number/s, and position of groups around ph-ring B linked to the thiadiazole ring.

2.3. Molecular Docking. Computational techniques found to be very effective in drug design and discovery have gained attention in the past few years, and these tools provide useful information about the discovered and target proteins. Consequently, it represents an effective way to know about the inhibition profile of the target proteins in a way that requires much less effort and cost. Additionally, to specify a potential hypothesis for the drug's mechanism of action (Table 2), the results of the docking of ligands **4**, **8**, **9**, and acarbose as a standard for α-glucosidase hydrolase PDB = 2BFH for the interaction of ligand and protein residue are shown. Docking score, energies, and root-mean-square deviation (RMSD) values are less than 3 Å, as shown in Table 3. Docking scores and energy varied somewhat around the values of acarbose. The sequence of values for acarbose, **4**, **8**, and **9** is −5.4386, −5.4792, 5.503, and −6.434, respectively, despite the fact that it has the highest value. 2D and 3D images of the complexes are shown (Figure 7).

Table 2. Docking Interactions of Selected Compounds with α-Glucosidase PDB = 2BFH

compound	ligand	receptor	interaction	distance E	(kcal/mol)
4	C 9	SG CYS 8 (A)	H-donor	3.72	−0.7
	N 18	CB CYS 8 (A)	H-acceptor	3.48	−0.5
8	6-ring	N THR 21 (A)	pi-H	4.46	−1.0
9	C 9	SG CYS 14 (A)	H-donor	3.65	−0.5
	S 12	O TYR 7 (A)	H-donor	3.82	−0.9
	N 14	CA GLN 13 (A)	H-acceptor	3.51	−0.7
acarbose	O 12	OE1 GLU 252 (B)	H-donor	3.11	−1.7
	O 21	OE1 GLU 252 (B)	H-donor	2.64	−2.3
	O 38	OE2 GLU 252 (B)	H-donor	2.73	−3.6
	O 61	OE1 GLU 252 (A)	H-donor	2.61	−3.2
	O 63	OD1 ASP 308 (B)	H-donor	2.84	−2.1
	O 77	OE2 GLU 312 (B)	H-donor	2.63	−4.6
	O 82	OD2 ASP 308 (B)	H-donor	2.75	−2.5
	O 86	OE2 GLU 312 (B)	H-donor	2.68	−3.5
	N 88	OE2 GLU 252 (B)	H-donor	2.90	−2.0
	O 61	NZ LYS 251 (A)	H-acceptor	2.95	−6.2

2.4. Pharmacokinetics. *2.4.1. ProTox-II.* The Protox-II virtual laboratory was used for the analysis of small molecule toxicities. Predicting compound toxicity is a crucial step in the development of new pharmaceuticals. In a rat model, the ProTox-II revealed that the three compounds are predicted to have oral LD_{50} values ranging from 159 to 2480 mg/kg, with quercetin having the lowest value and (1s, 4s)-Eucalyptol having the highest. For compounds **4**, **8**, and **9** (Table 4), the toxicity radar (Figure 8) is designed to quickly illustrate the confidence of positive toxicity results relative to the average of its class.

2.4.2. Pred-hERG. Biologically diverse protein targets are frequently bound by chemically related compounds, and protein structures cannot be recognized as alike ligands. Pharmacological and off-target relations between the proteins and a ligand set assist in boosting machine learning outcomes by interpolating the output prediction equalized by compound similarity development. This pipeline contributes to lowering false-negative errors and improving predictions of off-target drug effects. One of the key ideas in cheminformatics is chemical similarity. These similarity algorithm measurements are commonly calculated using the 2D Tanimoto method, which was applied in such cases. The final Tanimoto coefficient is fingerprint-based encoding every molecule to a fingerprint "bit" location (MACCS), with each bit recording whether or not a molecule fragment is present in the sample (1) or not (0). The results for potency are shown in Table 5.

2.4.3. DFT. Quantum chemical calculations were carried out in the current work to optimize the chosen structures by using the density functional theory (DFT)/B3LYP approach. In this

https://doi.org/10.1021/acsomega.3c05854
ACS Omega 2024, 9, 7480−7490

Table 3. Docking Score and Energy of Thiadiazole Derivatives with α-Glucosidase PDB = 2BFH

Cpd	S	RMSD-refine	E_conf	E_place	E_score1	E_refine	E_score2
4	−5.4386	1.8001	104.4704	−47.8666	−8.6447	−25.8635	−5.4386
8	−5.4792	1.5874	85.0759	−45.4296	−9.2677	−29.9352	−5.4792
9	−5.5030	1.8052	107.6404	−41.0920	−8.8630	−29.4637	−5.5030
acarbose	−6.4340	2.3285	252.1367	−92.8034	−11.4467	−35.3851	−6.4340

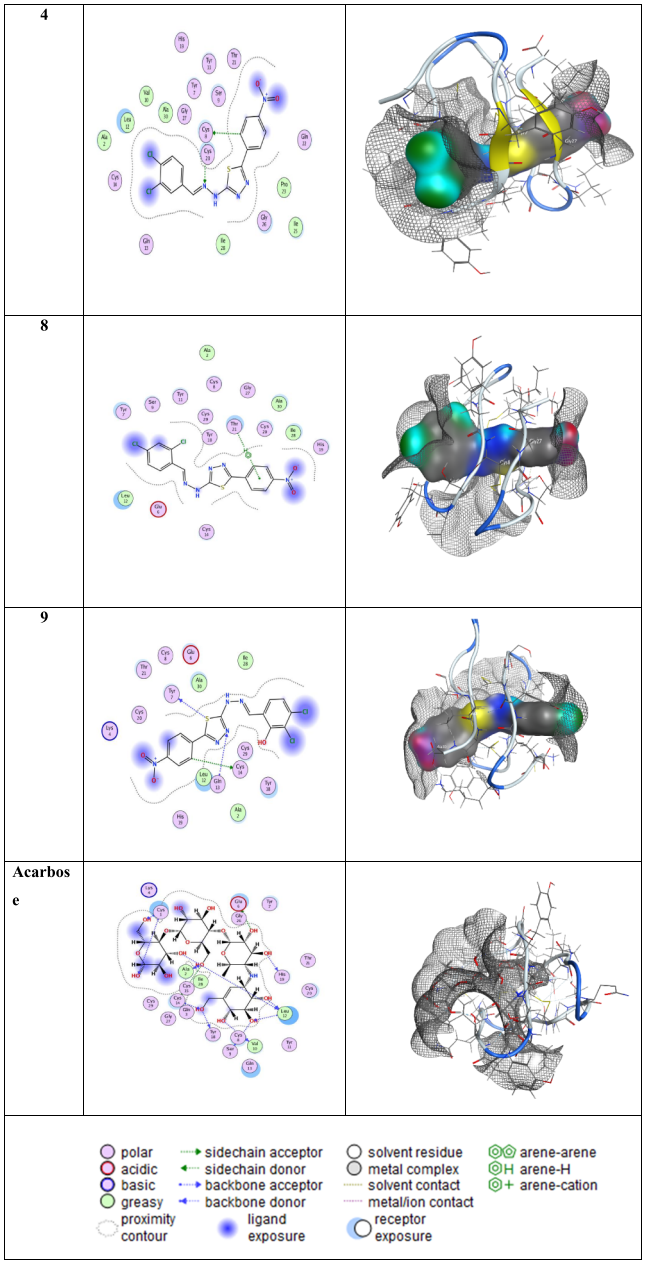

Figure 7. Interactions of thiadiazole derivatives with α-glucosidase PDB = 2BFH.

Table 4. Predicted Toxicity for 4, 8, and 9 Using ProTox-II

	4	8	9
Pro-ToxII			
predicted LD_{50} (mg/kg)	1200	1200	1200
predicted toxicity class	4	4	4
average similarity (%)	43.01	42.18	40.06
prediction accuracy (%)	54.26	54.26	54.26

test, the DFT (B3LYP) method using the 6-311G^{+2}(d,p) basis set was used. Figures 9 and 10 and Tables S1 and S2 show the optimized structure and its HOMO and LUMO values. The compound's capacity to act as an electron donor is expressed by the HOMO energy. Specifically, compounds **4**, **8**, and **9** are affected.

However, LUMO site energy may also serve as an electron attractive or electron acceptor. The compound electrostatic potential maps revealed regions of localized electrons throughout the molecules, with red and blue colors signifying, respectively, electron-rich (negative) and electron-deficient (positive) localization. Last but not least, the DFT calculations showed that the chosen compounds **4, 8,** and **9** had favorable energetic parameters, as shown in Table S2.

3. CONCLUSIONS

In conclusion, this work is carried out for the synthesis of 2-hydrazinyl-5-(4-nitrophenyl)-1,3,4-thiadiazole-bearing Schiff base derivatives and investigates their α-glucosidase inhibition profile. In the series (**1**−**12**), compounds are synthesized, and analogue **3** showed excellent inhibition against α-glucosidase enzymes in the range of IC_{50} value 18.10 ± 0.20 to 1.10 ± 0.10 μM. In this series, analogues **4, 8,** and **9** show remarkable inhibition profiles of IC_{50} 2.20 ± 0.10, 1.10 ± 0.10, and 1.30 ± 0.10 μM by using acarbose as a standard having an IC_{50} is 11.50 ± 0.30 μM. Furthermore, the docking score energies with RMSD value less than 3 Å, in contrast. The docking score energies varied somewhat around the values of acarbose. The sequence of values for acarbose **4, 8,** and **9** is −5.4386, −5.4792, 5.503, and −6.434, respectively, despite the fact that it has the highest value. With (1s, 4s)-Eucalyptol having the highest values and quercetin having the lowest compound, ProTox-II demonstrated that the three compounds are predicted to have oral LD_{50} values ranging from 159 to 2480 mg/kg in a rat model. Compounds **4, 8,** and **9** were categorically found to be moderate blockers with the potency of 5.858, 5.659, and 5.649, respectively. The selected compounds showed electrostatic potential maps revealed regions of localized electrons throughout the molecules, with two colors such as red and blue colors, respectively; electron-rich having negative charge and electron-deficient having positive charge localization on the basis of these results compounds **4, 8,** and **9** revealed favorable energetic parameters according to the DFT calculations. Upon the comparisons of other classes of compounds, none of the compounds showed a favorable α-glucosidase inhibition profile than the ones found in our work such as Cahyana et al., which synthesized **3** analogues and camphor-based analogues and assessed for α-glucosidase activity by using standard drug acarbose (IC_{50} = 859.06, >200, 1893.4, and 0.33 ppm),[41] another report by Olanipekun et al. synthesized the **1**−**6** compounds and assessed for α-glucosidase activity (IC_{50} = >600, 588.8 ± 3.84, 300.0 ± 0.95, 425.0 ± 0.97, 63.7 ± 0.52, 172.0 ± 0.36, 14.5 ± 0.15 μM, acarbose having an IC_{50} = 10.4 ± 0.06 μM),[42]

https://doi.org/10.1021/acsomega.3c05854
ACS Omega 2024, 9, 7480−7490

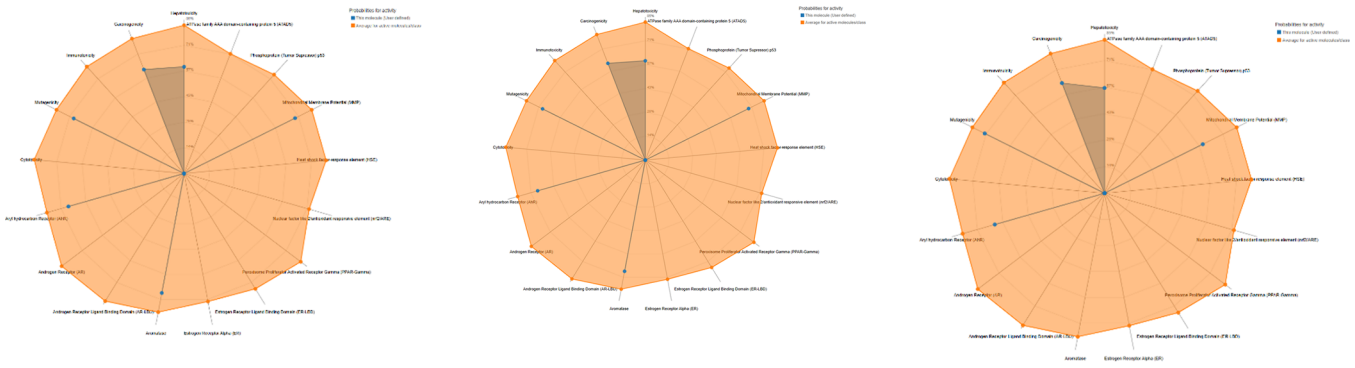

4 8 9

Figure 8. Confidence in positive toxicity results for compounds when compared to the class average.

Table 5. Predicted Pred-hERG Toxicity for 4, 8, and 9

no.	prediction	confiability %	applicability domain_n	categorical potency	confiability %	applicability domain_n	potency	applicability domain_n
4	nonblocker	53.71	outside	moderate blocker	36.98	outside	5.858	outside
8	nonblocker	87.1	outside	moderate blocker	34.75	outside	5.659	outside
9	nonblocker	90.76	outside	weak blocker	32.87	outside	5.649	outside

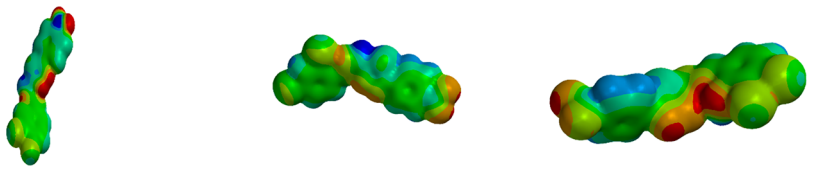

4 8 9

Figure 9. Electrostatic potential map of compounds **4**, **8**, and **9**.

and also another report by Fan et al. synthesized and evaluated their α-glucosidase activity.[43]

4. MATERIALS AND METHODS

Hydrazine hydrate, substituted benzaldehyde, 1,4-dioxane, and acetic acid were purchased from Sigma-Aldrich USA. Solvents were analytical grade, and reagents I_2, K_2CO_3, and other necessary solvents were purchased from local vendors and distilled before use if required. A Bruker Advance Av 600 MHz NMR spectrometer was used to simulate the spectra of ^{1}H NMR and ^{13}C NMR. The values of the simulated spectrum were expressed in hertz and parts per million, coupling constant (J), and chemical shift (δ). All the reactions were performed under air atmospheric pressure and checked through analytical techniques such as thin-layer chromatography on a precoated silica gel metal plate (E. Merck Germany). UV−visible (365 and 415 nm) lamp was used to visualize the spot on the TLC plates. A high-resolution electron ionization mass spectrum records the mass spectrum with m/z values.

4.1. General Procedure for the Synthesis of Thiadiazole-Based Schiff Base Analogues. In the first step, $N_2H_4.H_2O$ (a) was added to carbon disulfide in MeOH, and the reaction mixture was refluxed until conversion was complete (TLC was employed to check the conversion) to form thiocarbohydrazide (b). Substrate (b) was then subjected to 4-nitro-benzaldehyde in a methanolic solution along with a few drops of CH_3COOH, and the resulting residue was stirred at refluxing temperature to produce an intermediate (c), which further undergoes cyclization through an oxidative process in the presence of I_2 and K_2CO_3 in 1,4-dioxane to afford the synthesis of 2-hydrazino-1,3,4-thiadiazoles (d). In the next step, an intermediate (d) was reacted with different substituted benzaldehydes in acetic acid, and the resulting mixture was put on stirring under reflux to access the synthesis of desired 1,3,4-thiadiazole-based Schiff base analogues (**1**−**12**) (Scheme 1).

4.2. Characterization of Thiadiazole-Based Schiff Base Derivatives (1−12). Spectral analysis is provided in Supplementary File.

4.3. Assay Protocol for α-Glucosidase. Assay protocols for α-glucosidase were carried out in recent published work.[40,44]

4.4. Molecular Docking. Protein Data Bank (https://www.rcsb.org/) was used to locate the human pancreatic α-glucosidase with PDB ID: 2BFH. After using a large number of proteins, this one was ultimately selected to analyze interactions among the prepared ligands. The cocrystallized acarbose ligand acted as the control and was later isolated as a separate molecule, which was first used to retrieve the protein. Here, the Molecular Operating Environment (MOE) 2019 program was used.[45,46] Particular attention has been gained to this software's ability to dock prepared compounds into proteins.[47,48] Using the Quickprep tool, which is present in the MOE software, at a pH of 7, the structures were developed through the addition of hydrogen atoms while eliminating cocrystallized molecules and water. In a first step to confirm the docking process, the cocrystallized ligands were then redocked into the active sites with the target proteins. The remaining poses of the redocked ligands were overlaid on the cocrystallized ligands with RMSD values below 3 Å.[49] The

https://doi.org/10.1021/acsomega.3c05854
ACS Omega 2024, 9, 7480−7490

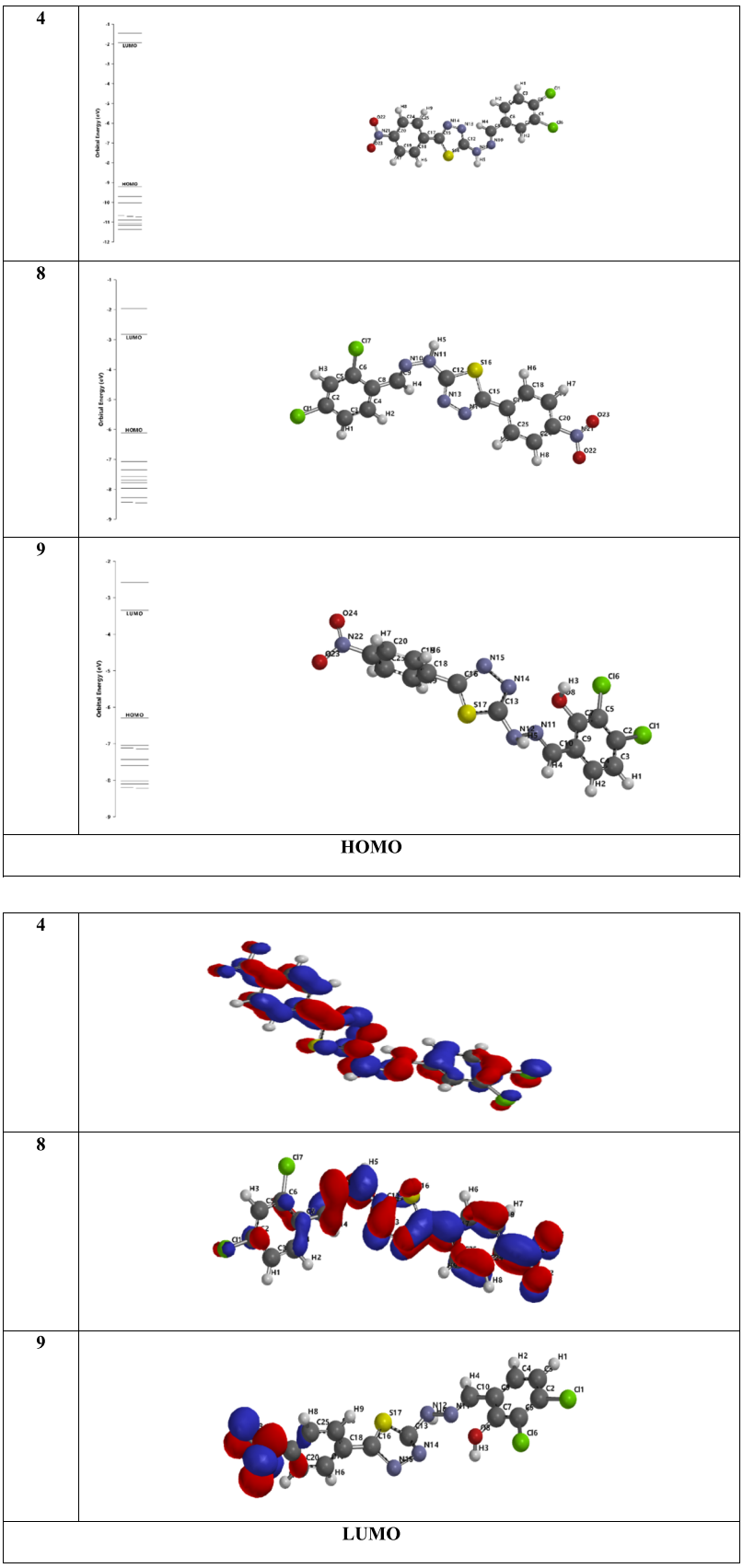

Figure 10. Optimized structure and its HOMO and LUMO of compounds **4**, **8**, and **9**.

poses of the targets and compounds were revealed by the docking results. From the more negative S-value, the most attractive pose was ranked, which is a computer-generated value for the binding's G (kcal.mol^{-1}) and has a low RMSD

https://doi.org/10.1021/acsomega.3c05854
ACS Omega 2024, 9, 7480−7490

Scheme 1. Synthesis of Thiadiazole-Bearing Schiff Base Derivatives

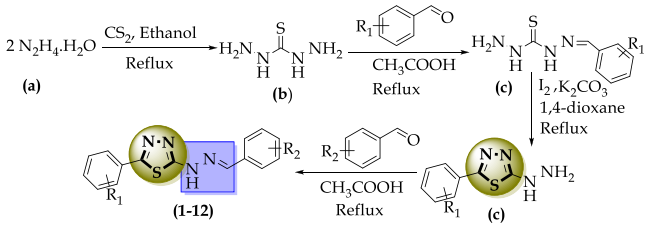

value (Å), which indicates that there was little perturbation during the docking process. To verify the stability of the binding and develop a "complex" (compound or target protein), these two parameters are recommended.

4.5. Pharmacokinetics. *4.5.1. LabMol and ProTox-II.* The number of animal experiments can be decreased using computational toxicity estimations, which are quicker than using animals to determine toxic doses. It is common to present toxic doses as LD_{50} in mg/kg body weight. The average dose, about 50% after testing of compounds, passes away after exposure to a substance. According to the globally standardized system of classification and labeling of chemicals, toxicity classes are established.[50,51] LD_{50} values are given in mg/kg.

Acute toxicity, hepatotoxicity, carcinogenicity, and mutagenicity are some of the toxicity end points that the ProTox-II software predicts.[52] The Pred-hERG program was used for the cardiotoxicity. It is based on the significantly important results predicted QSAR of hERG blockade more closely related to important deadly cardiac dysrhythmia (Table 6). The SDF and SMILES strings were adopted during the procedure.[53]

Table 6. Pharmacokinetics Study of the Synthesized Compounds

no.	class
1	class I: fatal if swallowed ($LD_{50} \leq 5$)
2	class II: fatal if swallowed ($5 < LD_{50} < 50$)
3	class III: toxic if swallowed ($50 < LD_{50} \leq 300$)
4	class IV: harmful if swallowed ($300 < LD_{50} \leq 2000$)
5	class V: may be harmful if swallowed ($2000 < LD_{50} < 5000$)
6	class VI: nontoxic ($LD_{50} > 5000$)

4.5.2. Molinspiration. 4.5.2.1. Bioavailability Radar. It is a technique for swiftly determining a molecule about drug-likeness. The following five physicochemical properties were selected, such as size, polarity, solubility, flexibility, and saturation. On each axis, a physicochemical range was assigned using the aforementioned descriptors[54] and shown as a pink area, into which the compounds' radar plot must entirely fall for the compound to be considered drug-like and used ProTox-II for their completion.

4.5.3. Physicochemical Properties. These include simple molecular and physical characteristics such as molecular weight (MW), the number of specific types of atoms, percentage of Csp3, and molecular refractivity that show the complexity of the molecule. Additionally, various absorption, distribution, metabolism, and excretion (ADME) features, such as those associated with passing through biological barriers, are performed through the reported work.[55]

4.5.4. Lipophilicity. The partition coefficient (Log Po/w) between n-octanol and water was used to describe it. Then, Molinspiration grants access to five free predictors performed through the literature-known method.[56]

4.5.5. Water Solubility. Water solubility is calculated by Molinspiration.[56] The decimal Log of *p* of the molar solubility in water and the Log of *S* values are the outcomes. Additionally, the water solubility in mg/mL and mol/L as well as the qualitative solubility classes were reported.

4.5.6. ADME Characteristics. Molinspiration uses customized models to evaluate the ADME characteristics of the test drugs. The "Lipinski Rule of Five" was invented in 1997 by Christopher A. Lipinski as a rule of thumb for evaluating drug-likeness and figuring out if an inhibitor with various biological and pharmacological properties would be an orally activated medication in the human body. The rule elaborates that a molecule can be orally absorbed/active if two (2) or more of the following conditions are fulfilled for the molecules such as MW (500), the octanol/water partition coefficient, nHBA_10, nHBD_5, and TPSA_40. For the blood−brain barrier first model is BBB for the penetration of gastrointestinal absorption,[57] while the second model is used for the status of permeability glycoprotein, which is required to calculate active efflux across membranes, such as from the gastrointestinal wall to the lumen or brain. CYP1A2, CYP2C19, CYP2C9, CYP2D6, and CYP3A4 are the primary sources of isoenzymes in cytochrome P450 (CYP), which are necessary for the transformational metabolic process and drug elimination. The third model foretells how drugs will interact with the enzymes. Additionally, the inhibition of these isoenzymes accelerates drug interactions that result in toxic or other negative outcomes. The skin permeability coefficient (K_p), which exhibits a linear relationship with both lipophilicity and molecule size, is predicted through the fourth model. Skin permeability declines with increasing log K_p (cm/s) negativity.[58]

4.6. Density Functional Theory. Quantum chemistry calculations were performed through the DFT technique using Spartan16 software. Additionally, all of the data files were displayed by applying Spartan16. The investigational compounds organic chemical structures were optimized using the DFT at 6-311G^{+2}(d,p) basis set/B3LYP method, and the original chemical structure was created using Chem3D 16.0 software.[59,60]

■ ASSOCIATED CONTENT

Supporting Information

The Supporting Information is available free of charge at https://pubs.acs.org/doi/10.1021/acsomega.3c05854.

Molecular orbital energy, atomic charges of compounds, spectroscopic data, and ^{1}H NMR spectra (PDF)

■ AUTHOR INFORMATION

Corresponding Author

Wajid Rehman − *Department of Chemistry, Hazara University, Mansehra 21120, Pakistan;* orcid.org/0000-0003-0128-0377; Email: sono_waj@yahoo.com

Authors

Zahid Ali − *Department of Chemistry, Hazara University, Mansehra 21120, Pakistan*

Liaqat Rasheed − *Department of Chemistry, Hazara University, Mansehra 21120, Pakistan*

https://doi.org/10.1021/acsomega.3c05854
ACS Omega 2024, 9, 7480−7490

Abdullah Y. Alzahrani − *Department of Chemistry, Faculty of Science and Arts, King Khalid University, Mohail, Assir 61421, Saudi Arabia*
Nawab Ali − *Shanghai Key Laboratory of Functional Materials Chemistry, School of Chemistry and Molecular Engineering, East China University of Science and Technology, Shanghai 200237, PR China*
Rafaqat Hussain − *Department of Chemistry, Hazara University, Mansehra 21120, Pakistan*
Abdul-Hamid Emwas − *Core Laboratories, King Abdullah University of Science and Technology (KAUST), Thuwal 23955-6900, Saudi Arabia*
Mariusz Jaremko − *Biological and Environmental Science and Engineering (BESE), King Abdullah University of Science and Technology (KAUST), Thuwal 23955-6900, Saudi Arabia*
Magda H. Abdellattif − *Department of Chemistry, Sciences College, Taif University, Taif 21944, Saudi Arabia;* orcid.org/0000-0002-8562-4749

Complete contact information is available at: https://pubs.acs.org/10.1021/acsomega.3c05854

Notes

The authors declare no competing financial interest.

■ ACKNOWLEDGMENTS

The authors extend their appreciation to the Deanship of Scientific Research at King Khalid University for funding this work through the large group Research Project under grant number (RGP2/413/44).

■ REFERENCES

(1) Kalidhar, U.; Kaur, A. 1, 3, 4-Thiadiazole derivatives and their biological activities: A Review. *Res. J. Pharm. Biol. Chem.* **2011**, *4*, 1091−1106.
(2) Serban, G.; Stanasel, O.; Serban, E.; Bota, S. 2-Amino-1, 3, 4-thiadiazole as a potential scaffold for promising antimicrobial agents. *Drug design, development and therapy* **2018**, 1545−1566.
(3) Jain, A. K.; Sharma, S.; Vaidya, A.; Ravichandran, V.; Agrawal, R. K. 1, 3, 4-Thiadiazole and its derivatives: A review on recent progress in biological activities. *Chemical biology & drug design* **2013**, *81* (5), 557−576.
(4) Wassel, M. M.; Ammar, Y. A.; Ali, G. A. E.; Belal, A.; Mehany, A. B.; Ragab, A. Development of adamantane scaffold containing 1, 3, 4-thiadiazole derivatives: Design, synthesis, anti-proliferative activity and molecular docking study targeting EGFR. *Bioorg. Chem.* **2021**, *110*, No. 104794.
(5) Vadakkedathu palakkeezhillam, V. N.; Haribabu, J.; Suresh kumar, V.; Manakkadan, V.; Rasin, P.; Bhuvanesh, N.; Echeverria, C.; Santibanez, J. F.; Sreekanth, A. Exploring the anticancer potential of thiadiazole derivatives of substituted thiosemicarbazones formed via copper-mediated cyclization. *Appl. Organomet. Chem.* **2023**, *37* (8), No. e7174.
(6) Hatami, M.; Basri, Z.; Sakhvidi, B. K.; Mortazavi, M. Thiadiazole−A promising structure in design and development of anti-Alzheimer agents. *International Immunopharmacology* **2023**, *118*, No. 110027.
(7) Hu, Y.; Li, C.-Y.; Wang, X.-M.; Yang, Y.-H.; Zhu, H.-L. 1, 3, 4-Thiadiazole: synthesis, reactions, and applications in medicinal, agricultural, and materials chemistry. *Chem. Rev.* **2014**, *114* (10), 5572−5610.
(8) Amir, M.; Kumar, A.; Ali, I.; Khan, S. A. Synthesis of pharmaceutically important 1, 3, 4-thiadiazole and imidazolinone derivatives as antimicrobials. *J. Chem.* **2009**, *41*, No. 201001138, DOI: 10.1002/chin.201001138.
(9) Salimon, J.; Salih, N.; Hameed, A.; Ibraheem, H.; Yousif, E. Synthesis and antibacterial activity of some new 1, 3, 4-oxadiazole and 1, 3, 4-thiadiazole derivatives. *J. of Applied Sciences Research* **2010**, *6* (7), 866−870.
(10) Oruç, E. E.; Rollas, S.; Kandemirli, F.; Shvets, N.; Dimoglo, A. S. 1, 3, 4-thiadiazole derivatives. Synthesis, structure elucidation, and structure− antituberculosis activity relationship investigation. *Journal of medicinal chemistry* **2004**, *47* (27), 6760−6767.
(11) Schenone, S.; Brullo, C.; Bruno, O.; Bondavalli, F.; Ranise, A.; Filippelli, W.; Rinaldi, B.; Capuano, A.; Falcone, G. New 1, 3, 4-thiadiazole derivatives endowed with analgesic and anti-inflammatory activities. *Bioorganic & medicinal chemistry* **2006**, *14* (6), 1698−1705.
(12) Labanauskas, L.; Kalcas, V.; Udrenaite, E.; Gaidelis, P.; Brukstus, A.; Dauksas, V. Synthesis of 3-(3, 4-dimethoxyphenyl)-1 H-1, 2, 4-triazole-5-thiol and 2-amino-5-(3, 4-dimethoxyphenyl)-1, 3, 4-thiadiazole derivatives exhibiting anti-inflammatory activity. *Die Pharmazie* **2001**, *56* (8), 617−619.
(13) Khalilullah, H.; Khan, M.; Mahmood, D.; Akhtar, J.; Osman, G. 1, 3, 4-Thiadiazole: A biologically active scaffold. *Int. J. Pharm. Pharm. Sci.* **2014**, *6* (9), 8−15.
(14) Husain, A.; Naseer, M. A.; Sarafroz, M. Synthesis and anticonvulsant activity of some novel fused heterocyclic 1, 2, 4-triazolo-[3, 4-b]-1, 3, 4-thiadiazole derivatives. *Acta Polym. Pharm.* **2009**, *66* (2), 135−140.
(15) Raj, V.; Rai, A.; Singh, M.; Kumar, A.; Kumar, V.; Sharma, S. Recent update on 1, 3, 4-thiadiazole derivatives: as anticonvulsant agents. *Am. Res. J. Pharm.* **2015**, *2* (1), 34−61.
(16) Clerici, F.; Pocar, D.; Guido, M.; Loche, A.; Perlini, V.; Brufani, M. Synthesis of 2-amino-5-sulfanyl-1, 3, 4-thiadiazole derivatives and evaluation of their antidepressant and anxiolytic activity. *Journal of medicinal chemistry* **2001**, *44* (6), 931−936.
(17) Anthwal, T.; Singh, H.; Nain, S. 1, 3, 4-thiadiazole scaffold: Anti-microbial agents. *Pharmaceutical Chemistry Journal* **2022**, *55* (12), 1345−1358.
(18) Muğlu, H.; Akın, M.; Çavuş, M. S.; Yakan, H.; Şaki, N.; Güzel, E. Exploring of antioxidant and antibacterial properties of novel 1, 3, 4-thiadiazole derivatives: Facile synthesis, structural elucidation and DFT approach to antioxidant characteristics. *Computational Biology and Chemistry* **2022**, *96*, No. 107618.
(19) Gowda, K.; Swarup, H. A.; Nagarakere, S. C.; Rangappa, S.; Kanchugarkoppal, R. S.; Kempegowda, M. Structural studies of 2, 5-disubstituted 1, 3, 4-thiadiazole derivatives from dithioesters under the mild condition: Studies on antioxidant, antimicrobial activities, and molecular docking. *Synth. Commun.* **2020**, *50* (10), 1528−1544.
(20) Pham, E. C.; Truong, T. N.; Dong, N. H.; Vo, D. D.; Hong do, T. T. Synthesis of a series of novel 2-amino-5-substituted 1, 3, 4-oxadiazole and 1, 3, 4-thiadiazole derivatives as potential anticancer, antifungal and antibacterial agents. *Medicinal Chemistry* **2022**, *18* (5), 558−573.
(21) Chandra sekhar, D.; Venkata rao, D.; Tejeswara rao, A.; Lav kumar, U.; Jha, A. Design and synthesis of 1, 3, 4-thiadiazole derivatives as novel anticancer and antitubercular agents. *Russian Journal of General Chemistry* **2019**, *89*, 770−779.
(22) Dou, L.; Shi, H.; Niu, X.; Zhang, H.; Zhang, K.; Wu, Z. Design, synthesis and antifungal mechanism of novel acetophenone derivatives containing 1, 3, 4-thiadiazole-2-thioethers. *New J. Chem.* **2022**, *46* (19), 9017−9023.
(23) Angeli, A.; Paoletti, N.; Supuran, C. T. Five-Membered Heterocyclic Sulfonamides as Carbonic Anhydrase Inhibitors. *Molecules* **2023**, *28* (7), 3220.
(24) Sidat, P. S.; Jaber, T. M. K.; Vekariya, S. R.; Mogal, A. M.; Patel, A. M.; Noolvi, M. Anticancer Biological Profile of Some Heterocylic Moieties-Thiadiazole, Benzimidazole, Quinazoline, and Pyrimidine. *Pharmacophore* **2022**, *13* (4), 59−71.
(25) Koçanci, F. G.; Aslim, B. Structure and functions of acetylcholinesterase and acetylcholinesterase inhibitory activity of plants. *Manas J. Agric. Vet. Life Sci.* **2016**, *6* (1), 19−35.

(26) Orhan, G.; Orhan, I.; Sener, B. Recent developments in natural and synthetic drug research for Alzheimer's disease. *Letters in Drug Design & Discovery* **2006**, *3* (4), 268−274.
(27) Gülsün inal, T.; Şahin, S. Diabetes and Diabetes Associated Physiologic and Pharmacokinetic Changes. *Hacet. Univ. J. Fac. Pharm.* **2017**, *37* (2), 105−123.
(28) Al-mosawy, M. Review of the biological effects of Schiff bases and their derivatives, including their synthesis. *Medical Science Journal for Advance Research* **2023**, *4* (2), 67−85.
(29) Singh, A.; Gogoi, H. P.; Barman, P.; Barman, P.; Singh, A.; Singh, A.; Gogoi, H. P.; Barman, P. General Applications of Schiff Bases and Their Metal Complexes. In *Schiff Base Metal Complexes: Synthesis and Applications*; Wiley, 2023; pp 119−128.
(30) Dudoit, A.; Benbouguerra, N.; Richard, T.; Hornedo-ortega, R.; Valls-fonayet, J.; Coussot, G.; Saucier, C. α-glucosidase inhibitory activity of Tannat grape phenolic extracts in relation to their ripening stages. *Biomolecules* **2020**, *10* (8), 1088.
(31) Anaya-isaza, A.; Zequera-diaz, M. Fourier transform-based data augmentation in deep learning for diabetic foot thermograph classification. *Biocybernetics and Biomedical Engineering* **2022**, *42* (2), 437−452.
(32) Dankner, R.; Roth, J. More recent, better designed studies have weakened links between antidiabetes medications and cancer risk. *Diabetic Medicine* **2020**, *37* (2), 194−202.
(33) Gummidi, L.; Kerru, N.; Ebenezer, O.; Awolade, P.; Sanni, O.; Islam, M. S.; Singh, P. Multicomponent reaction for the synthesis of new 1, 3, 4-thiadiazole-thiazolidine-4-one molecular hybrids as promising antidiabetic agents through α-glucosidase and α-amylase inhibition. *Bioorganic Chemistry* **2021**, *115*, No. 105210.
(34) Almandil, N. B.; Taha, M.; Rahim, F.; Wadood, A.; Imran, S.; Alqahtani, M. A.; Bamarouf, Y. A.; Ibrahim, M.; Mosaddik, A.; Gollapalli, M. Synthesis of novel quinoline-based thiadiazole, evaluation of their antileishmanial potential and molecular docking studies. *Bioorganic chemistry* **2019**, *85*, 109−116.
(35) Palamarchuk, I. V.; Shulgau, Z. T.; Dautov, A. Y.; Sergazy, S. D.; Kulakov, I. V. Design, synthesis, spectroscopic characterization, computational analysis, and in vitro α-amylase and α-glucosidase evaluation of 3-aminopyridin-2 (1 H)-one based novel monothioox-amides and 1, 3, 4-thiadiazoles. *Organic & Biomolecular Chemistry* **2022**, *20* (45), 8962−8976.
(36) Sherafati, M.; Mohammadi-khanaposhtani, M.; Moradi, S.; Asgari, M. S.; Najafabadipour, N.; Faramarzi, M. A.; Mahdavi, M.; Biglar, M.; Larijani, B.; Hamedifar, H. Design, synthesis and biological evaluation of novel phthalimide-Schiff base-coumarin hybrids as potent α-glucosidase inhibitors. *Chem. Pap.* **2020**, *74*, 4379−4388.
(37) Nasli-esfahani, E.; Mohammadi-khanaposhtani, M.; Rezaei, S.; Sarrafi, Y.; Sharafi, Z.; Samadi, N.; Faramarzi, M. A.; Bandarian, F.; Hamedifar, H.; Larijani, B. A new series of Schiff base derivatives bearing 1, 2, 3-triazole: Design, synthesis, molecular docking, and α-glucosidase inhibition. *Arch. Pharm.* **2019**, *352* (8), No. 1900034.
(38) Azizian, H.; Pedrood, K.; Moazzam, A.; Valizadeh, Y.; Khavaninzadeh, K.; Zamani, A.; Mohammadi-khanaposhtani, M.; Mojtabavi, S.; Faramarzi, M. A.; Hosseini, S. Docking study, molecular dynamic, synthesis, anti-α-glucosidase assessment, and ADMET prediction of new benzimidazole-Schiff base derivatives. *Sci. Rep.* **2022**, *12* (1), 14870.
(39) Tentolouris, A.; Vlachakis, P.; Tzeravini, E.; Eleftheriadou, I.; Tentolouris, N. SGLT2 inhibitors: a review of their antidiabetic and cardioprotective effects. *International journal of environmental research and public health* **2019**, *16* (16), 2965.
(40) Rasheed, L.; Rehman, W.; Rahim, F.; Ali, Z.; Alanazi, A. S.; Hussain, R.; Khan, I.; Alanazi, M. M.; Naseer, M.; Abdellattif, M. H. Molecular Modeling and Synthesis of Indoline-2, 3-dione-Based Benzene Sulfonamide Derivatives and Their Inhibitory Activity against α-Glucosidase and α-Amylase Enzymes. *ACS Omega* **2023**, *8* (17), 15660−15672.
(41) Cahyana, A. H.; Santika, G.; Phukan, K. Synthesis of camphor thiazole derivates from Dryobalanops aromatica and its bioactivity as antioxidants and antidiabetes against alpha glucosidase enzymes. *MethodsX* **2023**, *11*, No. 102429.
(42) Olanipekun, B. E.; Ponnapalli, M. G.; Patel, H. K.; Munipalle, K.; Shaik, K. Design, synthesis of new phenyl acetylene and isoxazole analogues of arjunolic acid as potent tyrosinase and alpha glucosidase inhibitors. *Natural Product Research* **2023**, *37* (7), 1092−1097.
(43) Fan, M.; Zhong, X.; Huang, Y.; Peng, Z.; Wang, G. Synthesis, biological evaluation and molecular docking studies of chromone derivatives as potential α-glucosidase inhibitors. *J. Mol. Struct.* **2023**, *1274*, No. 134575.
(44) Rahim, F.; Ullah, H.; Javid, M. T.; Wadood, A.; Taha, M.; Ashraf, M.; Shaukat, A.; Junaid, M.; Hussain, S.; Rehman, W. Synthesis, in vitro evaluation and molecular docking studies of thiazole derivatives as new inhibitors of α-glucosidase. *Bioorg. Chem.* **2015**, *62*, 15−21.
(45) Swilam, N.; Nawwar, M. A.; Radwan, R. A.; Mostafa, E. S. Antidiabetic activity and in silico molecular docking of polyphenols from Ammannia baccifera L. subsp. Aegyptiaca (Willd.) Koehne Waste: structure elucidation of undescribed acylated Flavonol Diglucoside. *Plants* **2022**, *11* (3), 452.
(46) Paşayeva, L.; Fatullayev, H.; Celik, I.; Unal, G.; Bozkurt, N. M.; Tugay, O.; Abdellattif, M. H. Evaluation of the chemical composition, antioxidant and antidiabetic activity of rhaponticoides iconiensis flowers: Effects on key enzymes linked to type 2 diabetes in vitro, in silico and on alloxan-induced diabetic rats in vivo. *Antioxidants* **2022**, *11* (11), 2284.
(47) Barakat, A.; Al-majid, A. M.; Soliman, S. M.; Lotfy, G.; Ghabbour, H. A.; Fun, H.-K.; Wadood, A.; Warad, I.; Sloop, J. C. New diethyl ammonium salt of thiobarbituric acid derivative: Synthesis, molecular structure investigations and docking studies. *Molecules* **2015**, *20* (11), 20642−20658.
(48) Abdellattif, M. H.; Shahbaaz, M.; Arief, M.; Hussien, M. A. Oxazinethione derivatives as a precursor to pyrazolone and pyrimidine derivatives: Synthesis, biological activities, molecular modeling, ADME, and molecular dynamics studies. *Molecules* **2021**, *26* (18), 5482.
(49) Cheng, F.; Li, W.; Zhou, Y.; Shen, J.; Wu, Z.; Liu, G.; Lee, P. W.; Tang, Y. admetSAR: a comprehensive source and free tool for assessment of chemical ADMET properties. *J. Chem. Inf. Model.* **2012**, *52*, 3099−3105, DOI: 10.1021/ci300367a.
(50) Erhirhie, E. O.; Ihekwereme, C. P.; Ilodigwe, E. E. Advances in acute toxicity testing: strengths, weaknesses and regulatory acceptance. *Interdisciplinary toxicology* **2018**, *11* (1), 5−12.
(51) El-din, H. M. A.; Loutfy, S. A.; Fathy, N.; Elberry, M. H.; Mayla, A. M.; Kassem, S.; Naqvi, A. Molecular docking based screening of compounds against VP40 from Ebola virus. *Bioinformation* **2016**, *12* (3), 192.
(52) Banerjee, P.; Eckert, A. O.; Schrey, A. K.; Preissner, R. ProTox-II: a webserver for the prediction of toxicity of chemicals. *Nucleic acids research* **2018**, *46* (W1), W257−W263.
(53) Barros, J. C. M. *Mining cardiac side-effects of known drugs*; JCM Barros, 2015.
(54) Daina, A.; Michielin, O.; Zoete, V. SwissADME: a free web tool to evaluate pharmacokinetics, drug-likeness and medicinal chemistry friendliness of small molecules. *Sci. Rep.* **2017**, *7* (1), 42717.
(55) Murad, H. A. S.; Alqurashi, T. M. A.; Hussien, M. A. Interactions of selected cardiovascular active natural compounds with CXCR4 and CXCR7 receptors: A molecular docking, molecular dynamics, and pharmacokinetic/toxicity prediction study. *BMC Complementary Med. Ther.* **2022**, *22* (1), 35.
(56) Sharma, D.; Singh, V. Isolation of Bioactive Compounds from Fruit Body of Lentinula edodes (Berk.) Pegler and In Silico Approach using Tyrosinase Target Protein Involved in Melanin Production. *Indian J. Pharm. Sci.* **2022**, *84*, 1026−1040.
(57) Shanmugapriya, S. *Amelioration of Neuroprotective Effect of Semisynthetic Derivatives of Piperine in Rotenone induced Rat Model of Parkinson's Disease*; College of Pharmacy, Sri Ramakrishna Institute of Paramedical Sciences, 2021.

https://doi.org/10.1021/acsomega.3c05854
ACS Omega 2024, 9, 7480−7490

(58) Wang, N.-N.; Wang, X.-G.; Xiong, G.-L.; Yang, Z.-Y.; Lu, A.-P.; Chen, X.; Liu, S.; Hou, T.-J.; Cao, D.-S. Machine learning to predict metabolic drug interactions related to cytochrome P450 isozymes. *J. Cheminf.* **2022**, *14* (1), 1−16.
(59) Ito, K.; Obuchi, Y.; Chikayama, E.; Date, Y.; Kikuchi, J. Exploratory machine-learned theoretical chemical shifts can closely predict metabolic mixture signals. *Chemical science* **2018**, *9* (43), 8213−8220.
(60) Nevriansyah, E.; Frissherly, A.; Mathriu, A. Q.; Putri, U. N.; Handri, S. A Bioinformatics Research of Active Compounds Curcuma xanthorriza in Arthritis Disease. *ARITMETIKA* **2022**, *1* (01), 26−33.

https://doi.org/10.1021/acsomega.3c05854
ACS Omega 2024, 9, 7480−7490